CHARACTERISATION OF HIGH PRESSURE DIESEL FUEL SPRAYS BY ENTROPIC EDGE DETECTION

P. L. Luque Escamilla[1], J. Seneschal[2], J.F. Gomez Lopera[3], C.Ducottet[2], J. Martinez Aroza[3], J. C. Champoussin[4]
peter@ujaen.es
jerome.seneschal@univ-st-etienne.fr

[1] Universidad de Jaén
C/ Alfonso X El Sabio 28. 23700 Linares. Jaén. Spain
[2] LTSI (Laboratoire Traitement du Signal et Instrumentation)
UMR CNRS 5516, 23 rue du docteur Paul Michelon, 42023 Saint-Etienne Cedex 02, France
[3] Universidad de Granada
Campus Fuente Nueva. 18071 Granada. Spain
[4] LMFA (Laboratoire de Mécanique des Fluides et d'Acoustique)
UMR CNRS 5509, ECL, 36 avenue Guy de Collongue, BP 163, F-69131 ECULLY cedex, France

Abstract
This paper presents an edge detector using the Jensen-Shannon divergence of grey level histograms obtained by sliding a double window over an image. A new technique for linking unconnected edge points, based on estimated directions, is also described. An application of edge extraction for diesel spray images is shown. From this segmentation of the spray, the spray tip penetration can be measured. This information is an important parameter to improve combustion in diesel engine.

Introduction

The air/fuel mixing process in a diesel engine combustion chamber determines the combustion itself and the pollutants emissions. The quality of the ready-to-burn mixture depends on the high pressure fuel spray evolution, in terms of tip penetration, cone angle and local atomisation. The knowledge of these parameters will help the manufacturer to improve their fuel injection system and provides data to the researcher in order to increase its understanding on the process. To get this information on the spray, non-intrusive optical diagnostics are of prime interest [1]. But due to the unsteadiness of the phenomenon, a lot of images may be recorded, from which by a statistical analysis based on specific images processing, we can give a description of the jet. To do that efficiently, we need first of all a fully automated edge detection contour [2]. This paper is devoted to the application of the Entropic edge detection concept to the characterisation of high pressure diesel fuel sprays. It is composed of three parts : the experimental set up to collect the images, the implementation of the Jensen-Shannon criteria to extract the parameters and finally the results with regards to the spray tip penetration.

Experimental setup

First of all, it should be specified that all the experiments have been performed with ISO 4113 proof oil, which is very similar to diesel fuel as about density and viscosity.

The classical Common Rail system includes a fuel pump, which can raise the Injection Pressure (IP) up to 135 MPa and a common-rail tank, with an internal volume of 45 mm^3 which supplies oil to the injector under test. For our experiment, we use a VCO (Valve Covered Orifice) nozzle injector with five holes of diameter 150 µm The length of each hole is around 600µm and one hole is perpendicular to the axis, the others are drilled on a spiral below.

The oil discharges at atmospheric pressure in a transparent chamber designed to operate safely as shown in Figure 1. The injector axe is oriented horizontally to avoid the injected fluid deposition on the horizontal viewing faces. No vertical deflection of the spray has been observed. So we can conclude that gravity does not disturb the spray shape. White light sources illuminate the scene and we observed scattered light by the sprays. Images are recorded by a CCD intensified camera with resolution 1024×1280 pixels and aperture time of 100 ns. Between the beginning of the Injection Control Signal (ICS) and the effective beginning of the needle, which is a good indication of the Start Of Injection (SOI), there is a delay called Needle Opening Time Delay (NOTD) as we can see on the chronogram in Figure 2. This delay is due to the electromechanical characteristics of the injector and to the internal fluid behaviour (compressibility). The higher the injection pressure is, the shorter the NOTD. In our future spray tip penetration representation, we will use the beginning of the ICS as reference time.

A specific electronic control unit controls the injection timing and duration, the injected quantity, the rail pressure and synchronizes the camera.

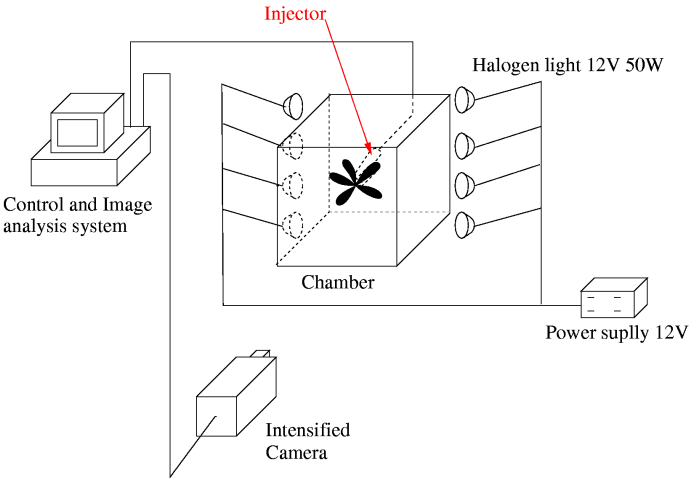

Figure 1. Schematic illustration of the experimental setup

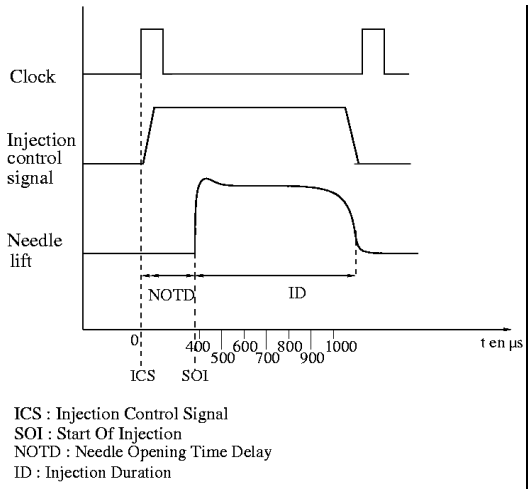

Figure 2. Chronogram of the injection process.

Edge detection method

Edge detection: Jensen Shannon divergence

Jensen-Shannon divergence (hereafter JS), proposed by Lin [3], has proved to be a powerful tool in the segmentation of digital images and applications [4][5]. It is a measurement of the inverse cohesion of a set of probability distributions Pi having the same number of possible realizations :

$$JS_{\pi}(P_1, P_2, ..., P_r) \equiv H\left(\sum_{i=1}^{r} \pi_i P_i\right) - \sum_{i=1}^{r} \pi_i H(P_i), \quad (1)$$

where $P_1, P_2, .., P_r$ are discrete probability distributions $P_i = \{P_{i,j} \,/\, j = 1, ..., n\}$, $i = 1, ..., r$, $\pi \equiv \left\{\pi_1, \pi_2, ..., \pi_r \,/\, \pi_i > 0, \sum_{i=1}^{r} \pi_i = 1\right\}$ are the distribution weights for Pi, and $H(P_i) = -\sum_{j=1}^{n} P_{i,j} \log P_{i,j}$ is the Shannon entropy.

Divergence grows as the differences between its arguments (the probability distributions involved) increase, and vanishes when all the probability distributions are identical. The application of JS to edge-detection is based on a three-step structured procedure as follows [4].

Calculation of divergence and direction matrices

Let us consider a window made up of two identical subwindows and sliding down over a straight edge between two different textures as in Figure 3, in this case r = 2 in eq. (1). It has been shown [4] that in such conditions JS of the normalized histograms of the subwindows reaches its maximum value when each subwindow lies completely within one texture.

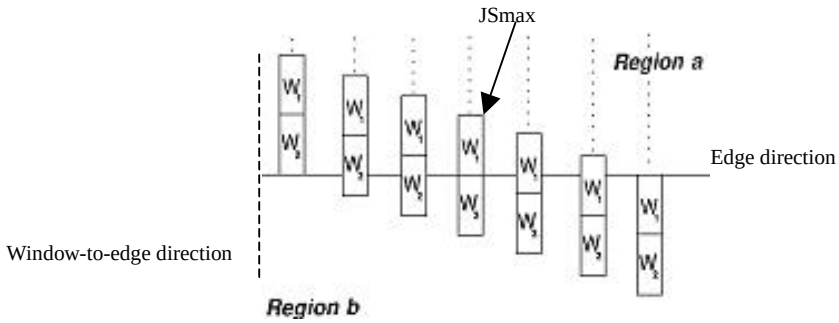

Figure 3. A window sliding across a perfect straight edge.

If the window-to-edge direction is not perpendicular, JS maxima reaches lower values that may be close to zero and then undetectable. This means we need to try several window orientations. For each pixel of the image, four orientations of the window-to-edge direction are technically possible: vertical, horizontal and the two

diagonals. The maximum JS obtained with these four windows centered on the pixel of interest allows to build a matrix of real numbers called divergence matrix.

At the same time the direction of the edge —*i.e.* the direction where JS reaches its maximum— is estimated from the periodical behavior of JS with the window orientation and interpolating from the four JS_i available. The direction that maximizes JS results to be $\delta = \pi x \in [0, \pi)$, where *x* verifies:

$$\begin{aligned}
&\text{if } JS_1 - JS_3 \geq 0,\ JS_2 - JS_4 \geq 0 \quad \Rightarrow x = \frac{JS_2 - JS_4}{4[(JS_1 - JS_3) - (JS_2 - JS_4)]} \in [0, 1/4] \\
&\text{if } JS_1 - JS_3 \geq 0,\ JS_2 - JS_4 \leq 0 \quad \Rightarrow x = \frac{4(JS_1 - JS_3) - 3(JS_2 - JS_4)}{4[(JS_1 - JS_3) - (JS_2 - JS_4)]} \in [3/4, 1] \\
&\text{if } JS_1 - JS_3 \leq 0,\ JS_2 - JS_4 \geq 0 \quad \Rightarrow x = \frac{2(JS_1 - JS_3) - (JS_2 - JS_4)}{4[(JS_1 - JS_3) - (JS_2 - JS_4)]} \in [1/4, 1/2] \\
&\text{if } JS_1 - JS_3 \leq 0,\ JS_2 - JS_4 \leq 0 \quad \Rightarrow x = \frac{2(JS_1 - JS_3) + 3(JS_2 - JS_4)}{4[(JS_1 - JS_3) - (JS_2 - JS_4)]} \in [1/2, 3/4]
\end{aligned} \tag{2}$$

The empirical error in the determination of x is never greater than 0.004. Thus, a direction matrix is then built with the δ's value.

Obtaining edge pixels

Thresholding the divergence matrix [4][6] is not always useful for decide which pixels form the divergence matrix are edge pixels, since maximum JS values depend on the composition of adjacent textures, and will thus vary according to texture. Consequently, it would seem more appropriate to use a local criterion. Accordingly, each edge-pixel candidate is the centre of an odd-length monodimensional window, perpendicularly placed to the estimated edge direction in that pixel (from the direction matrix). The condition for being an edge pixel is then:

$$JS_{central} - JS_j \geq T_d \tag{3}$$

for any other pixel j in that particular monodimensional window, where T_d is a threshold. Pixels marked as edge pixels are then outstanding local maxima of the divergence matrix. Obviously, detection results depend directly on the parameter T_d, which can be modified by the user if necessary.

This local edge-pixel detection method requires simple divergence matrix pre-processing. Small fluctuations, often due to noise in the original image or to texture regularity, can introduce a great number of false maximums, although they are usually fairly low. The divergence matrix is therefore smoothed out by repeatedly applying a 3×3 mean filter.

Selection of a local maximum is, in a sense, a thinning procedure since just one pixel will usually be detected as an edge pixel within the neighborhood, as determined by the size of the monodimensional window. In fact, rarely would more than one pixel share the same maximum JS.

It must be said, however, that direct application of the above method does not provide good results for some kinds of images —corrupted by Gaussian noise, or with regions having small fluctuations in grey levels— because the JS could be too sensitive to any change in grey levels between regions. It is therefore better to construct the divergence matrix including extra information in addition to the histogram information using the following expression:

$$JS^*_{i,j} = JS_{i,j}\left(1 - \alpha + \alpha W_{i,j}\right), \tag{4}$$

where $W_{i,j} = \frac{|N_{w1} - N_{w2}|}{N_w}$, N_{w1} and N_{w2} being the average grey levels of subwindows W_1 and W_2, and N_w the maximum grey level inside the window (normalization factor). $\alpha \in [0,1]$ is the attenuation factor, which determines the weights of JS and the grey levels inside the window. This modification makes the JS suitable for different kinds of images, thus transforming our algorithm into a hybrid among texture-based algorithms [7], Jensen-Shannon divergence [6] and grey-level based algorithms (gradient, Laplacian, Laplacian and gradient of the Gaussian, etc [8]).

Edge linking

The two steps described above make it possible to extract the image edge pixels. However, it is not always feasible to establish a good compromise between the quality of the binary image obtained and the desired

connectivity of the edge pixels, possibly due to the presence of noise in the original image, and the texture composition of the image regions. In order to deal with these problems, a third step can be added: edge-pixel linking. This step attempts to join the various sets of edge pixels using information from the divergence matrix associated with the image, together with knowledge of the direction in which maximum JS is produced. In broad terms, the linking procedure consists in extracting edge pixels unmarked since they did not satisfy the condition (3), but nearly did. Not all the pixels in the image are candidates for filling the gaps, only those classified as neighbor candidates of end pixels.

The definition of end pixel in [9] includes several variants that may influence the result of the linking process. The present paper uses the definition of end pixel as a pixel having one or two marked pixels joined together. Thus, only certain neighbor end pixels are candidates for prolonging image edges. In Figure 4 we present the candidate pixels for containing a given edge. For a given neighbor candidate to be marked as an edge pixel, it must satisfy two conditions:

- Its associated JS must be reasonably high. The first prolongation condition is then:

$$JS_{end} - JS_{neigbhour-candidate} \leq \tau_d \,, \tag{5}$$

  where τ_d is a threshold, which has at first no relation with parameter T_d in step 2 of the procedure.

- The estimated edge-direction of the end pixel ($\mathrm{Dir}_{\mathrm{end}}$), the edge-direction neighbor candidate ($Dir_{neighbour-candidate}$) and the direction of the physical line joining them ($Dir_{end,\,\mathrm{neighbour\text{-}candidate}}$) must not differ by more than a specified amount. The second prolongation condition is then:

$$\begin{aligned}&\left(Dir_{end,\,\mathrm{neighbour\text{-}candidate}} - \mathrm{Dir}_{\mathrm{end}}\right)^2 \\ &+\left(Dir_{end,\,\mathrm{neighbour\text{-}candidate}} - Dir_{neighbour-candidate}\right)^2 \leq \tau_\theta\end{aligned}, \tag{6}$$

  where τ_θ is another threshold.

The two foregoing conditions are used in an attempt to extract as edge pixels those pixels lying next to end pixels and whose JS and direction are sufficiently close to those of the end pixel to be extended. It should be borne in mind that when a new pixel is marked as an edge, other adjacent pixels can then become end pixels. So, the algorithm must foresee this event in order to continue the search for links.

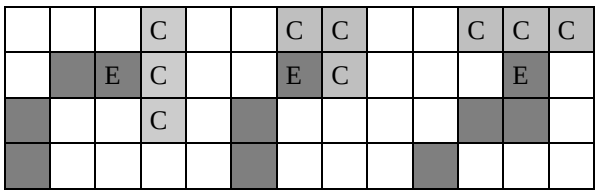

Figure 4. End points and neighbour candidates for edge prolongation. E: end point. C: neighbour candidates. The remaining grey pixels are edge pixels.

Final considerations about edge detection procedure Typical usual parameters values

This section briefly summarizes all the parameters used by the edge-detection procedure. Initially, the proposed segmentation procedure may seem difficult to use due to the elevated number of parameters that user can vary. But in practice the procedure is easy to use because all the images are similar. In the table below we present the typical parameter values used in this work.

	Parameter value	Symbols	Typical value
Step 1	Sliding window size		3×3
	Attenuation coefficient	α	0.75
Step 2	Monodimensional window size		11
	Mean filter iterations		8
	Local maximum selection threshold	T_d	0.7
Step 3	Divergence threshold	τ_d	0.1
	Direction threshold	τ_θ	0.5

Main results

First hybrid texture based algorithm developed above is compared to the more classical grey level based algorithms of Canny. Then the hybrid algorithm is used for injector design from tip penetration measurements.

Edge detection quality/reliability

The following images show the results of the proposed edge detection method applied to sprays from a five holes injector under IP = 80 MPa. Our camera allows us to take only one image at a given instant of injection. For five successive injections, five images are recorded at the same instant of the injection. Then the edge detection by the Jensen-Shannon divergence method is computed on the average image of the spray at each instant. Figure 7 shows the detected spray boundaries overlaid on the original average image of Figure 5.

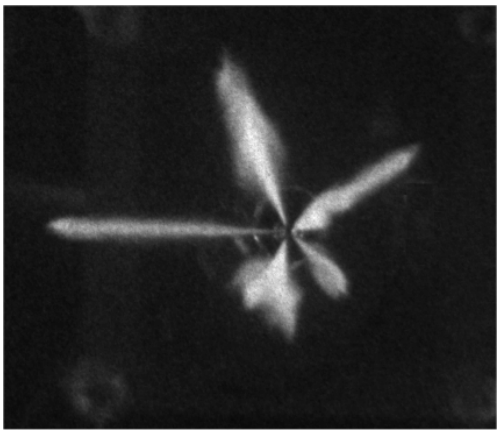

Figure 5. Average image at a given instant of an injection shot (IP = 80 MPa) : here 590 µs after SOI.

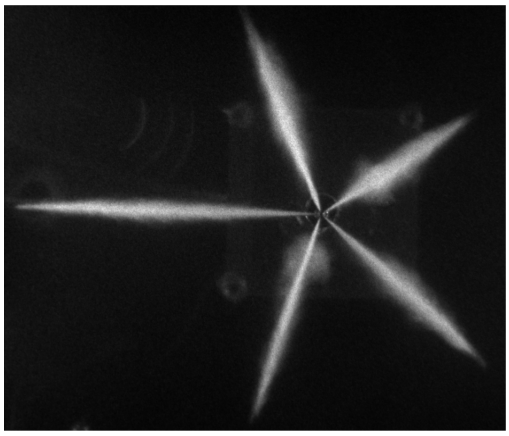

Figure 6. Average image at a given instant of an injection shot (IP = 80 MPa): here 1070 µs after SOI

We can see that the Jensen-Shannon method not only can extract the edges of the spray but gives also different brightness areas due to the scattered light by the sprays. The peripheral areas of the spray are grey while the central parts are very bright. The algorithm allows detecting the limits of these different areas within the sprays.

From the average image (Figure 5), the gradient based algorithm of Canny [10] was implemented. Previously, a Gaussian filter was applied to this image to reduce the noise. Then the Canny filter is computed. The result is given in the Figure 7.

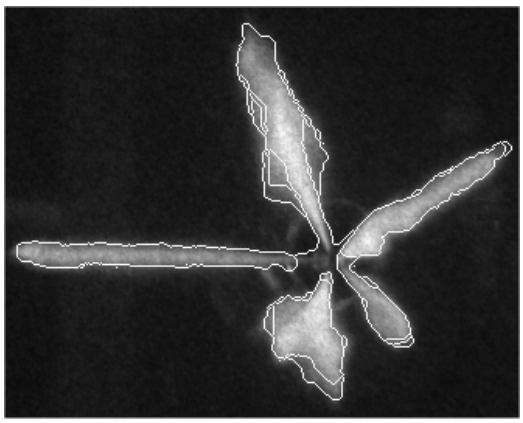

Figure 7. Superposition of the average image (Figure 5) and of the edges detected by the JS algorithm. 590 µs after SOI .

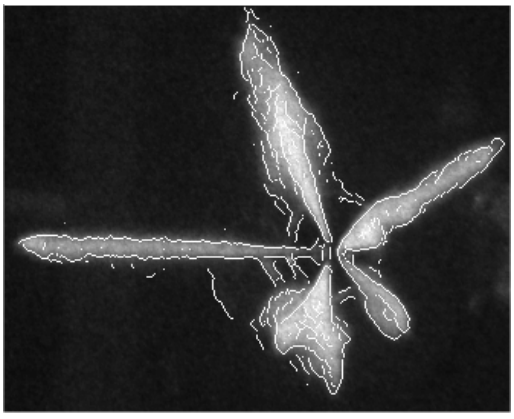

Figure 8. Superposition of the average image (Figure 5) and of the edges detected when using Canny filter. 590 µs after SOI.

When comparing figures 7 and 8, we can see that the Jensen-Shannon segmentation gives results more reliable than other methods based on the Gaussian gradient operator, such as the Canny filter.

Designing features

Analysing the evolution with time of the average images like in figure 5, hole-to-hole variations may be observed in terms of spray angle and spray penetration, especially for initial development of the spray. From the figures 5 and figure 6, it appears that later in the injection shot, hole-to-hole spray variability of VCO nozzle disappeared. This observation is confirmed by the measurement of the spray tip penetration using the edge

extract by the Jensen Shannon method. The two following charts show the penetration of the five sprays for two different injection pressure (40 and 80 MPa).

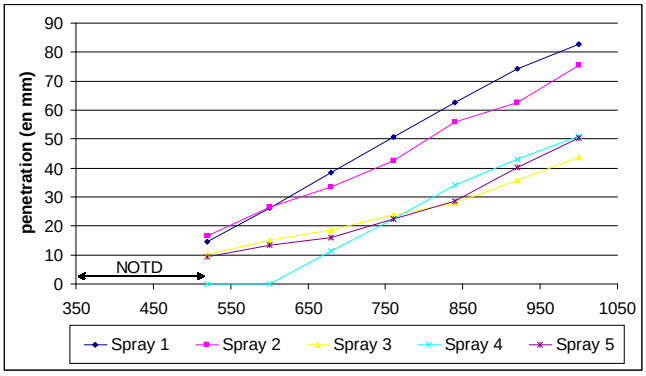

Figure 8. Spray tip penetration (40 MPa).

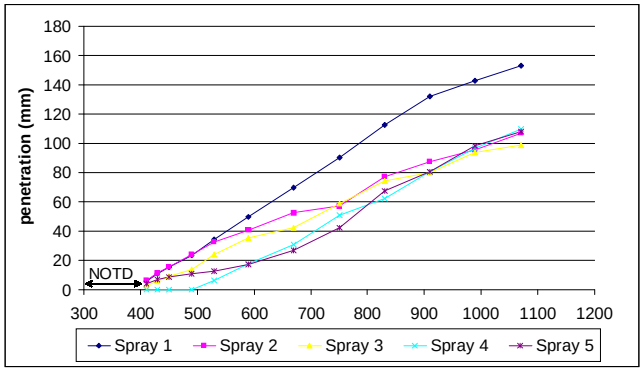

Figure 9. Spray tip penetration (80 MPa).

At the first stage of injection, spray tip penetrations are closely related to their patterns. The penetration varies significantly depending on the spray. However, at about 900 ms after the SOI, at 80 MPa, four sprays reach the similar values, only spray 1 keeps a higher penetration, at 40 MPa, spray 1 and 2 on one hand and spray 3, 4, and 5 on the other hand, reach similar values, but different for the two groups. This information is of interest for the designer of the nozzle in order to get a homogeneous distribution of fuel droplets.

Conclusion

This paper deals basically with a method for the extraction of edge pixels, corresponding to the maxima of the Jensen-Shannon divergence of the histograms of two subwindows. The method has been improved in an hybrid procedure among texture-based algorithms, Jensen-Shannon divergence and grey-level based algorithms Additionally, a new algorithm is presented for edge linking using the same entropic technique.

This method was successfully applied on sprays images of a five-hole VCO nozzle of Common Rail system. Not only the edges of the five sprays can be extract showing their different evolutions with time, but also different brightness areas within the sprays giving more reliable results than Canny method.

A hole-to-hole spray variability in terms of spray angle and spray penetration has been observed, especially for initial development. This observation is confirmed for two injection pressure by the measurement of the spray tip penetration using the edge extract by the JS method. An increase of pressure decreases the variability. All these information are valuable for the designer of the nozzle in order to get a homogeneous distribution of the fuel droplets to improve the mixture with air, and forward for the combustion process.

The next step will be the automation of the procedure.

References

[1] N. Bochard, I. Baz, C. Ducottet, T. Boedec, P. Gucher, J.C. Champoussin, J.P. Schon, “Nouvelle Techniques de Visualisation Appliquées à l’Etude de l’Injection Diesel Haute Pression”, *Photoniques*, 4, 26-28, (December 2001).

[2] J. Seneschal, C. Ducottet, N. Bochard, P. Gucher, J.C. Champoussin,“Visualization of High Pressure Diesel Sprays from Single and Multi-Hole Injectors”, *FISITA 2002*, Helsinki, FINLAND, June 2002.

[3] J. Lin,“Divergence Measures based on the Shannon Entropy”, *IEEE Transactions of Information* Theory, 37 1, 145-150, (1991).

[4] V. Barranco Lopez, P.L. Luque Escamilla, J. Martinez Aroza, R.R. Roman Roldan, “Entropic Texture Edge Detection for Image Segmentation”, *Electronics Letters*, 31 11, 1867-869, (1995).

[5] C. Atae Allah, M. Cabrerizo Vílchez, J.F. Gómez Lopera, J. Holgado Terriza, P.L. Luque Escamilla, R.R. Roman Roldan, “Measurement of surface tension and contact angle using entropic edge detection”, *Measurement Science and Technology*, 12 288-298 (2001).

[6] J.F. Gomez Lopera, A.M. Robles Pérez, J. Martínez Aroza, R. Román Roldán, “ An analysis of edge detection by using the Jensen-Shannon divergence”, *J. Math. Imaging Vision*, 13, 35-56 (2000).

[7] D.J. Park, K. M. Nam, R. H. Park, “Edge-detection in noisy images based on the co-occurrence matrix” *Pattern Recognition Letters*, 27 6, 765-775 (1994).

[8] Pratt W. *Digital Image Processing.* Wiley-Interscience (1994).

[9] L. Lam, “Thinning Methodologies-A Comprehensive Survey” *IEEE Transactions on Pattern Analysis and Machine Intelligence*, PAMI 14 9, (1992).

[10] J. Canny, “A computational Approach to Edge Detection” *IEEE Transactions on Pattern Analysis and Machine Intelligence*, PAMI 8 6, (1986).